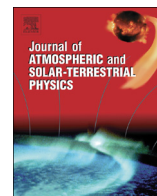




Contents lists available at ScienceDirect

Journal of Atmospheric and Solar-Terrestrial Physics

journal homepage: www.elsevier.com/locate/jastp

Wavelength dependence of solar irradiance enhancement during X-class flares and its influence on the upper atmosphere

Yanshi Huang^{a,*}, Arthur D. Richmond^b, Yue Deng^c, Phillip C. Chamberlin^d, Liying Qian^b, Stanley C. Solomon^b, Raymond G. Roble^b, Zuo Xiao^e^a Department of Electrical and Computer Engineering, University of New Mexico, NM, USA^b High Altitude Observatory, National Center for Atmospheric Research, Boulder, CO, USA^c Department of Physics, University of Texas at Arlington, TX, USA^d Solar Physics Laboratory, NASA Goddard Space Flight Center, Greenbelt, MD, USA^e Department of Geophysics, Peking University, Beijing, China

ARTICLE INFO

Article history:

Received 26 April 2013

Received in revised form

25 September 2013

Accepted 11 October 2013

Keywords:

Solar flare

FISM

TIE-GCM

ABSTRACT

The wavelength dependence of solar irradiance enhancement during flare events is one of the important factors in determining how the Thermosphere–Ionosphere (T–I) system responds to flares. To investigate the wavelength dependence of flare enhancement, the Flare Irradiance Spectral Model (FISM) was run for 61 X-class flares. The absolute and the percentage increases of solar irradiance at flare peaks, compared to pre-flare conditions, have clear wavelength dependences. The 0–14 nm irradiance increases much more (~680% on average) than that in the 14–25 nm waveband (~65% on average), except at 24 nm (~220%). The average percentage increases for the 25–105 nm and 122–190 nm wavebands are ~120% and ~35%, respectively. The influence of 6 different wavebands (0–14 nm, 14–25 nm, 25–105 nm, 105–120 nm, 121.56 nm, and 122–175 nm) on the thermosphere was examined for the October 28th, 2003 flare (X17-class) event by coupling FISM with the National Center for Atmospheric Research (NCAR) Thermosphere–Ionosphere–Electrodynamics General Circulation Model (TIE-GCM) under geomagnetically quiet conditions ($K_p=1$). While the enhancement in the 0–14 nm waveband caused the largest enhancement of the globally integrated solar heating, the impact of solar irradiance enhancement on the thermosphere at 400 km is largest for the 25–105 nm waveband (EUV), which accounts for about 33 K of the total 45 K temperature enhancement, and ~7.4% of the total ~11.5% neutral density enhancement. The effect of 122–175 nm flare radiation on the thermosphere is rather small. The study also illustrates that the high-altitude thermospheric response to the flare radiation at 0–175 nm is almost a linear combination of the responses to the individual wavebands. The upper thermospheric temperature and density enhancements peaked 3–5 h after the maximum flare radiation.

© 2013 Elsevier Ltd. All rights reserved.

1. Introduction

A solar flare results from a sudden, intense release of magnetic energy in the atmosphere of the Sun, which produces rapid increases in electromagnetic radiation, from gamma rays to radio wavelengths (Einar and Gordon, 1988). Flares are classified as A, B, C, M, or X according to the maximum flux of 0.1–0.8 nm X-rays measured near the Earth (Garcia, 2000). While C-class flares are a common occurrence during years near solar maximum, the

frequency of X-class flares during solar maximum is approximately two per month (<http://spacemath.gsfc.nasa.gov>). There are large spectral variations among flares (Thomson et al., 2004; Tsurutani et al., 2005; Chamberlin et al., 2012). The enhancement of the Extreme Ultraviolet (EUV, ~25 to ~120 nm) spectral irradiance depends on the location of a flare, whereas the flare enhancement of X-ray Ultraviolet (XUV, ~0.1 to ~25 nm) radiation depends only weakly on location (Qian et al., 2010).

Solar EUV photons are the primary energy source of the neutral and ionized constituents of the Thermosphere–Ionosphere (T–I) system (Mitra, 1974; Liu et al., 2011). The extra ionization in the ionosphere caused by flares increases electron density, which influences the absorption and refraction of radio waves propagating through the ionosphere from one station to another (Einar and Gordon, 1988). Also, flares are often associated with Coronal Mass Ejections (CMEs), which may cause significant geomagnetic storms

* Corresponding author. Tel.: +1 7349722340.

E-mail addresses: huangys@unm.edu, yanshi.huang@mavs.uta.edu (Y. Huang), richmond@hao.ucar.edu (A.D. Richmond), yuedeng@uta.edu (Y. Deng), phillip.c.chamberlin@nasa.gov (P.C. Chamberlin), lqian@ucar.edu (L. Qian), stans@ucar.edu (S.C. Solomon), roble@hao.ucar.edu (R.G. Roble), zxiao@pku.edu.cn (Z. Xiao).

(Munro et al., 1979; Harrison, 1987; Tsurutani et al., 1988; Gonzalez et al., 1994; Michalek, 2009; Bein et al., 2012). Previous studies have shown that the impact of flares on the T-I system varies because flares have different magnitudes, locations on the solar disk, rise rates and decay rates (Tsurutani et al., 2005; Sutton et al., 2006; Qian et al., 2010, 2011; Zhang et al., 2011, 2012). Since XUV dominates ionization in the lower thermosphere (< 150 km), and EUV dominates in the upper thermosphere (Qian et al., 2011), the impact of solar flares on the upper atmosphere depends on the solar irradiance enhancement at different wavelengths.

The purpose of this paper is to investigate how different wavebands of solar irradiance are enhanced during flares and how they impact the global thermosphere. The Flare Irradiance Spectral Model (FISM) (Chamberlin et al., 2007, 2008) was employed to estimate the spectra of solar irradiance. The National Center for Atmospheric Research (NCAR) Thermosphere-Ionosphere-Electrodynamics General Circulation Model (TIE-GCM) (Roble et al., 1988; Richmond et al., 1992) driven by the FISM was used to simulate the thermospheric responses to flares.

2. Model description

2.1. Flare irradiance spectral model (FISM)

FISM is an empirical model of the solar irradiance spectrum from 0.1 to 190 nm at 1 nm resolution and on 1-minute time cadence. The high temporal resolution of FISM makes it possible to study the variations due to solar flares. This model is based on the data provided by the Solar Extreme ultraviolet Experiment (SEE) (Woods et al., 2005) on the Thermosphere Ionosphere Mesosphere Energetics and Dynamics (TIMED) satellite, and the SOLAR STellar Irradiance Comparison Experiment (SOLSTICE) (Rottman, 2000) on the Solar Radiation and Climate Experiment (SORCE).

FISM estimates the daily component of irradiance, including the variations from the solar cycle and solar rotation of active regions (Chamberlin et al., 2007). The flare component of FISM includes both the impulsive and gradual phase variations, and is based on a reference set of 39 large flares from 2002 to 2005 measured by SEE and SORCE (Chamberlin et al., 2008). This reference set of measurements is fit to a flare proxy to determine the coefficients. The Geostationary Operational Environmental Satellites (GOES) 0.1–0.8 nm fluxes are used as the flare proxy to empirically model the flare variation for FISM, because of its high temporal resolution and reliable data since 1970 with few data gaps, as well as plans for continued future measurements. A linear relation is found between the irradiance of GOES 0.1–0.8 nm and the irradiance for the X-rays at wavelengths less than 14 nm, while a power law relation with exponent of 0.647 is found between the irradiance of GOES 0.1–0.8 nm and the irradiance for EUV at wavelengths larger than 14 nm (Chamberlin et al., 2008).

Due to large variations during flares for different wavelengths, and due to limited measurements, the FISM flare uncertainty has a wavelength dependence that varies from 10% to above 100%. However, compared to models with only daily outputs, FISM improves the estimation of solar flares significantly. More flare data can help reduce the FISM flare uncertainties. The newly available and more accurate data from the Extreme ultraviolet Variability Experiment (EVE) on the Solar Dynamics Observatory (SDO) (Woods et al., 2010, 2011) will add the additional variable of temporal delays in some of the EUV emissions during the gradual phase of flares (Chamberlin et al., 2012).

2.2. NCAR TIE-GCM

The NCAR TIE-GCM is a first-principles, three-dimensional, non-linear representation of the coupled thermosphere and ionosphere

system. It solves the momentum, energy and continuity equations for neutral and ion species in pressure coordinates (Roble et al., 1988), with a self-consistent calculation of ionospheric wind dynamo effects (Richmond et al., 1992). The external forcings of TIE-GCM are mainly the solar irradiance, magnetospheric energy, and tidal perturbations at the lower boundary of the model. Magnetospheric energy inputs include auroral particle precipitation and high-latitude ion convection. In this study, the Heelis potential model (Heelis et al., 1982) was used to specify the high-latitude electric field while the auroral particle precipitation is as described by Roble and Ridley (1987). The latest version (v1.94) of the TIE-GCM was run with a $5^\circ \times 5^\circ \times$ half scale height resolution (longitude \times latitude \times vertical).

Solar irradiance spectra estimated by the FISM were used as solar input to the TIE-GCM in our study. The spectral range required by the TIE-GCM is 0.05–175 nm, so the part of FISM spectra at wavelengths greater than 175 nm is not included. The low-resolution binning scheme developed by Solomon and Qian (2005) is utilized to separate the FISM spectrum into 37 bins for the solar EUV energy deposition calculation. The spectrum between 0.05–105 nm is divided into 22 non-uniform bins according to the changes of cross sections and photon energy within a bin. The part of spectra with wavelengths longer than 105 nm is divided evenly into 5-nm bins except for the Lyman- α line (121.56 nm) (Qian, 2007).

The heating due to solar irradiance from 0.05 to 105 nm is calculated through integrating heating over the first 22 bins as shown by Wang (1998) in Eq. (2.8), which depends on the solar flux at different wavelengths, the ionization cross sections of N_2 , O_2 , and O, and the column number densities of N_2 , O_2 , and O. The contribution of the Schumann–Runge continuum (105–175 nm) is integrated over the remaining 15 bins. The photodissociation by radiation in the Schumann–Runge continuum is the primary direct dissociation process for O_2 in the thermosphere. The excess energy from O_2 dissociation goes directly into heating, which is about 6.6% of the absorbed Schumann–Runge radiation (Schunk and Nagy, 2009). The quenching process of $O(^1D)$ resulted in the O_2 dissociation also contributes to the neutral heating. The neutral gas heating by the Schumann–Runge bands is specified by the empirical formula in Strobel (1978), with a heating efficiency of about 0.3.

3. Results and discussion

3.1. Solar irradiance enhancements from the FISM for X-class flares

A flare is classified as A, B, C, M or X according to the peak flux of 0.1–0.8 nm irradiance near the Earth. Within each class, a linear scale from 1.0 to 9.9 is used to specify the magnitude of a flare, except for X-class flares, the class number can exceed 9.9. The biggest flare in the National Oceanic and Atmospheric Administration (NOAA) records is an X28 flare that occurred on November 4, 2003. The November 4, 2003, flare saturated GOES X-ray sensor (XRS), and its magnitude was initially estimated as X28 through extrapolating the GOES curve (<http://www.swpc.noaa.gov>). Thomson et al. (2004) argued that the magnitude of this X28 flare should be as large as X45.5 based on the measurements of ionospheric VLF (Very Low Frequency) radio phase change.

Fig. 1 depicts the FISM outputs for the X17 flare on October 28th, 2003 (day of year 301). The top panel shows the temporal variation of total solar flux integrated over 0–190 nm wavelengths, which started to increase at 11:00 UT and reached a maximum flux of 100 mW/m² at around 11:07 UT. Solar spectra before the flare and at the flare peak are shown in the middle panel. The black line is for the pre-flare time which is marked with a triangle in the top panel, whereas the red line is for the time at the flare peak which

Download English Version:

<https://daneshyari.com/en/article/8140214>

Download Persian Version:

<https://daneshyari.com/article/8140214>

[Daneshyari.com](https://daneshyari.com)